Annals of Biomedical Engineering, Vol. 8, pp. 75-92, 1980
Printed in the USA.
0090-6964/80/010075-18 $02.00/0

THE EFFECTS OF HIP CONTACT ABERRATIONS ON STRESS PATTERNS WITHIN THE HUMAN FEMORAL HEAD

Thomas D. Brown
and
Albert B. Ferguson, Jr.

Department of Orthopaedic Surgery
University of Pittsburgh
Pittsburgh, Pennsylvania

A two-dimensional finite element model incorporating cancellous bone inhomogeneity is used to study femoral head stress alterations caused by changes from the usual articular contact patterns. The contact stress distributions, calculated from an earlier mathematical analysis by Greenwald and O'Connor (16), are found to influence not only the adjacent subchondral bone, but relatively distant parts of the head as well. Both abnormally large joint incongruity and abnormally low cartilage compliance cause load to shift away from the superior "weight-bearing" area, out toward the periphery of the contact region. As a consequence, transverse compressive stresses, which are of appreciable magnitude but which do not contribute to weight bearing, are built up throughout much of the superior and central portions of the femoral head. Most small changes in the overall cartilage thickness or in its thickness distribution, when considered in isolation from hip compliance changes, have only minor effects on the internal stress distribution. An important exception is cartilage thinning at the superior margin, which can result in abrupt longitudinal compressive stress concentrations. It is suggested that such alterations of the normal patterns of stress transmission may contribute to sclerosis or to the formation of osteophytes or cysts in the osteoarthritic hip.

The long-term integrity of the human femoral head as a weight-bearing organ is often subject to compromise by degenerative changes, particularly those of osteoarthritis. Aberrant patterns of articular surface loading clearly affect the mechanical stress state in the underlying articular cartilage and subchondral bone (24). Interestingly, both abnormally high (13) and ab-

This study was aided by grants from the Easter Seal Research Foundation (#N7739), the National Science Foundation (#ENG78-05451), the Barra Foundation, Inc., and the Western Pennsylvania Chapter of the Arthritis Foundation. The authors wish to acknowledge the excellent service provided by the University of Pittsburgh Computer Center. The assistance of Mr. Gary E. Graf and Mrs. Diana W. Montgomery are also appreciated.

Requests for reprints may be sent to Thomas D. Brown, Orthopaedic Research Laboratory, 986 Scaife Hall, University of Pittsburgh, Pittsburgh, Pennsylvania 15261.

normally low (7) stress levels have been implicated in the pathogenesis of osteoarthritis. But the extent to which contact stress pattern alterations influence the stress field within the femoral head as a whole is not well understood. An appreciation of this relationship may prove important, because the complex patterns of trabeculation will be altered to accommodate an abnormal stress state. And, since local regions of high elastic modulus within an epiphyseal region have been shown to transmit elevated stresses (3), the initial aberrant contact stress patterns may become self-sustaining. In the present study, a two-dimensional inhomogeneous finite-element model is used to evaluate the stress distribution changes within the femoral head resulting from a series of perturbations in the articular contact stress. The stress perturbations arise from variations (*1*) in the total hip loading, (*2*) in the degree of incongruity in the non-weight-bearing hip, (*3*) in the minimum cartilage thickness, (*4*) in the distribution of cartilage thickness, and (*5*) in the overall femoral head deformation under load.

Bullough et al. (6,7), and Greenwald and associates (14,15,16) have conducted extensive studies of contact areas in the human hip, using injected dye to stain cartilage in the noncontact areas. Their results clearly demonstrate that the femoral head cartilage underlying the dome of the acetabulum of a normal hip comes into contact only during the high-force portions of the loading cycle. By contrast, cartilage underlying the periphery of the acetabulum is habitually in contact. These phenomena are consistent with observations showing that the radius of curvature of the (somewhat asperical) acetabulum is slightly smaller than that of the (very nearly spherical) femoral head (2). Interestingly, Bullough et al. (6) have found that the asphericity of the acetabulum decreases significantly with increasing age. Measurements by P.S. Walker et al. (33) have shown that the maximal subdome gap in the normal unloaded young adult hip is only 0.5 mm, suggesting that the geometrical tolerances affecting hip mechanics are small indeed.

To date, there have been only indirect measurements of the distribution of articular contact stresses in the natural hip (9), although ultraminiature piezoresistive transducers suitable for direct measurements have been recently developed (5). Greenwald and O'Connor (16), however, have presented a simplified mathematical contact stress analysis which is consistent with dye injection contact area data. Their results for contact stress in terms of initial joint congruity, cartilage thickness distribution, and overall hip compliance provide a convenient basis from which the internal stress pattern alterations can be explored.

METHOD

The finite element technique has emerged as an important tool in the study of mechanical stresses in articular joints, due to the highly irregular geometries, material property distributions, and boundary conditions encountered in such structures. The need for improvements in total hip arthro-

plasty design and fixation has motivated a series of increasingly complex finite element models of the proximal femur (1,8,18,26,27,29,32), including recently the treatment of material inhomogeneity and fully three-dimensional geometry. In studies of the significance of several independent physical variables, however, it is often practical to sacrifice some numerical precision by adopting a simplified formulation, in order to undertake reasonably economical parametric evaluations. In the present study, a two-dimensional plane stress formulation was chosen in lieu of axisymmetry (because of the roughly 30° misalignment between the axes of loading versus geometrical symmetry) and in lieu of plane strain (because out-of-plane deformations are of the same order as those in-plane). Clearly, the results thus obtained are not strictly applicable to the three-dimensional, physiological configuration; rather, they apply only to a thin section, loaded in-plane, whose geometry and material properties are those of a coronal midsection.

The plane stress finite element analysis was implemented using the eight-node curved quadrilateral isoparametric "serendipity" element first described by Ergatoudis et al. (10). For a direct stiffness, plane stress formulation, the nodal interpolation function N_i for this element is given for corner nodes by

$$N_i = \tfrac{1}{4}(1+\xi\xi_i)(1+\eta\eta_i) - \tfrac{1}{4}(1-\xi^2)(1+\eta\eta_i) - \tfrac{1}{4}(1+\xi\xi_i)(1-\eta^2), \tag{1}$$

where ξ and η denote the local natural coordinates, and the subscript describes the node number. The local stiffness matrices,

$$[k] = \int\int [B]^T [D] [B] \, dx \, dy \tag{2}$$

are evaluated by numerical integration (19), with the strain-displacement matrix $[B]$ calculated in terms of the coordinate transformation Jacobian. Inhomogeneities in the elasticity matrix $[D]$ were incorporated in the model, based upon our measurements of the spatial variations of the cancellous bone material properties (4), and Kempson's et al. (20) measurements of cartilage stiffness distributions. A coronal section 3 mm anterior to the fovea capitis was chosen for study, and was zoned into finite elements, in the manner shown in Fig. 1. The numerical value within each element indicates the average (isotropic) elastic modulus value assigned to that particular element.

The distributions of articular contact stress for the finite-element study were calculated from the simplified axisymmetrical model of Greenwald and O'Connor (16), in which the femoral head was taken to be a sphere of radius R, and the acetabulum to be an ellipsoid of revolution with a semiminor axis also of R. Under the assumption that surface deformation at any point of contact was dependent only on the normal stress acting at that point

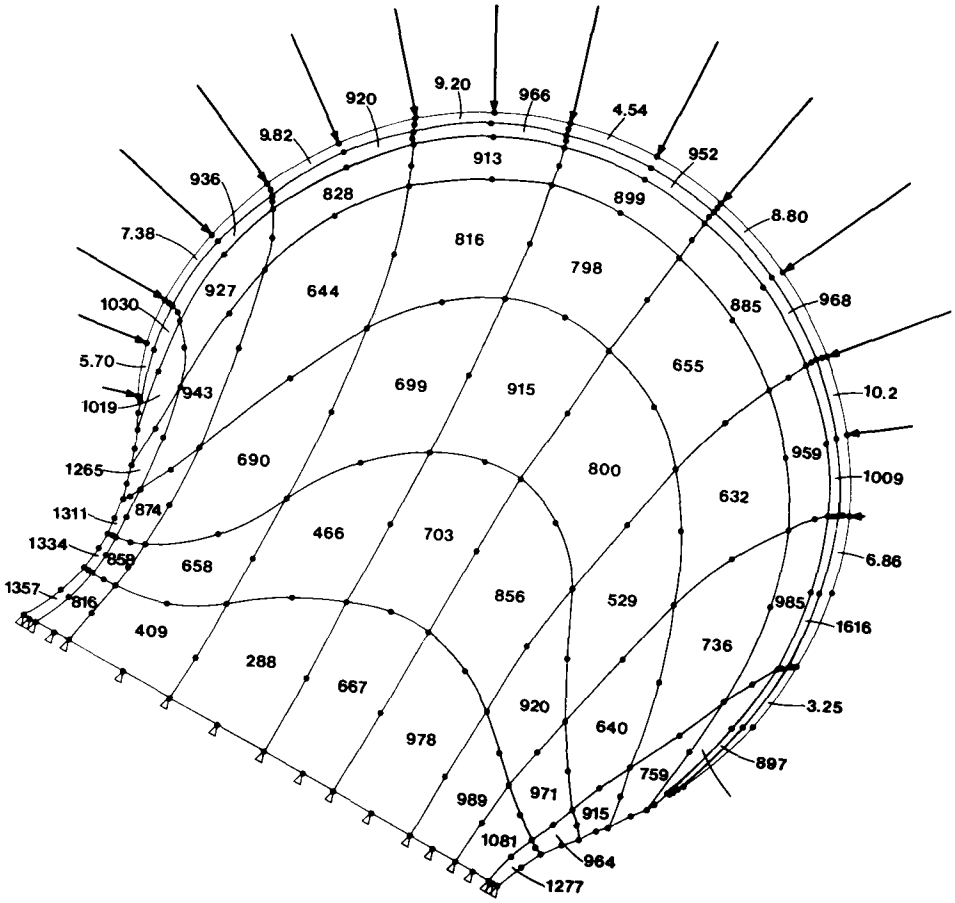

FIGURE 1. Finite element discretization and boundary conditions for the femoral head study section. There are 63 curvilinear elements, each of which has four corner nodes and four midside nodes (444 global degrees of freedom). The articular loading acts normal to the surface, and has discretized values (at the contact nodes) which are proportional to the arrow lengths. The zero-displacement distal boundary condition is symbolized by the open triangles. The elastic modulus values assigned to the individual elements are indicated in MN/m².

(i.e., a "bedspring" model), they calculated that, for an ideally lubricated surface, the normal contact stress σ_r would be given by

$$\sigma_r(\phi) = \frac{F}{2\pi R^2} \cdot \frac{d/d_0 - \cos\phi}{h_0/h_1 + \cos\phi} \cdot \cos\phi \cdot \frac{1}{A} , \tag{3}$$

where F is the total hip load, d_0 is the gap under the acetabular dome in the absence of loading, and d is the deflection caused by application of the force F (see definition sketch, Fig. 2). The cartilage thickness, h, is taken to be composed of a uniform thickness component, h_0, and a nonuniform component h_1:

$$h = h_0 + h_1 \cos\phi . \tag{4}$$

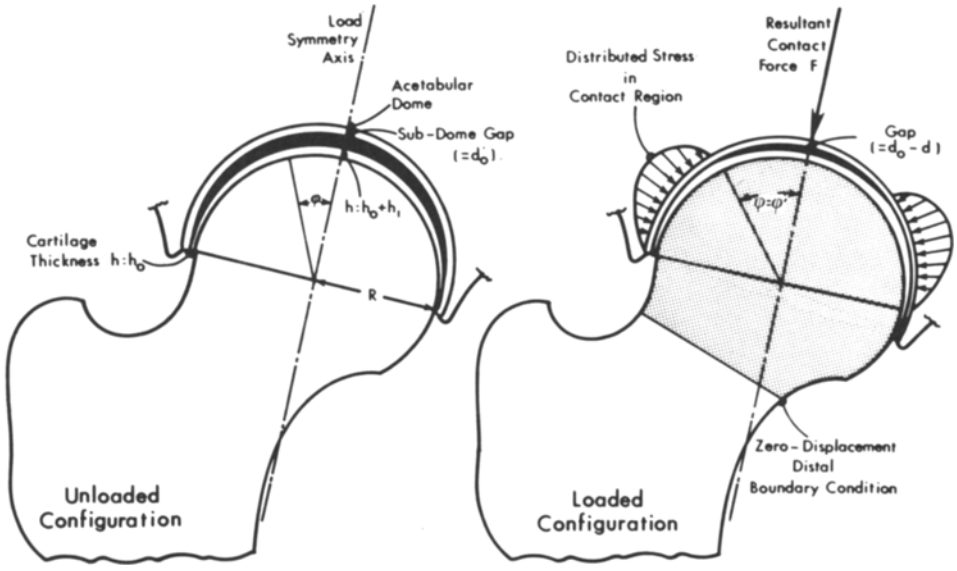

FIGURE 2. Geometrical definition sketch. The angular displacement ϕ is measured from the load symmetry axis. The dot-shaded region in the right-hand figure denotes the finite element study region.

In Eqs. 3 and 4, ϕ is the local angular displacement (assuming spherical symmetry) measured from a reference line passing through the acetabular dome and the geometrical center of the femoral head. For complete contact, the symbol A denotes the expression

$$A = \frac{d}{d_0}\left[\frac{1}{2} - \frac{h_1}{h_0} + \left(\frac{h_0}{h_1}\right)^2 \ln\left(1 + \frac{h_1}{h_0}\right)\right] - \left[\frac{1}{3} - \frac{1}{2}\frac{h_0}{h_1} + \left(\frac{h_0}{h_1}\right)^2 - \left(\frac{h_0}{h_1}\right)^3 \ln\left(1 + \frac{h_1}{h_0}\right)\right], \tag{5}$$

while in the contact region ($\phi \geqslant \phi'$, see Fig. 2b) of a hip with incomplete contact

$$A = \frac{1}{6}\left(\frac{d}{d_0}\right)^3 - \frac{1}{2}\frac{h_0}{h_1}\left(\frac{d}{d_0}\right)^2 + \left(\frac{h_0}{h_1}\right)^2 \times \frac{d}{d_0}\left[\ln\left(1 + \frac{h_1}{h_0}\frac{d}{d_0}\right) - 1\right] + \left(\frac{h_0}{h_1}\right)^3 \ln\left(1 + \frac{h_1}{h_0}\frac{d}{d_0}\right). \tag{6}$$

In the present study, the contact stresses in the two-dimensional coronal study section (which contains the axis about which the contact stresses were assumed to be symmetrical) were taken to be equal to those determined by Greenwald and O'Connor's (16) axisymmetrical analysis.

In view of the large spatial gradients of articular contact stress which can arise from Eqs. 3–6, the usual consistent nodal load allocation procedure

(37) was replaced by a more intuitive one. The load acting at each contact node was taken to be the surface integral of all (normal) contact stress acting on a tributary region, bounded on the left and right by points halfway to the neighboring nodes, surrounding the contact node. Although this intuitive allocation procedure involved a small loss in accuracy of stress in the first (i.e., cartilage) element layer for elements well within the contact region, it had the advantages of providing a more precise resolution of the contact/noncontact interface, and of providing nodal loading vectors which were directed more nearly normal to the articular surface in the interface region (particularly for cases of large stress gradients near the interface). A zero-displacement boundary condition was assumed for nodes across the bottom (distal neck) section (refer to Fig. 1), while a zero-net-force boundary condition was assumed for the exterior nodes at the medial and lateral margins.

The patterns of load transmission at various points in the normal walking cycle (21) were studied by prescribing serial increases in the total joint load force F, while the deflection d varied in accordance with experimentally measured load/deflection curves for the normal hip (16). To examine the effects of various degrees of acetabular incongruity, changes were prescribed in the initial subdome gap d_0. Uniform cartilage thickness variations were modelled by variations in the coefficient h_0, while changes in the distribution of femoral head cartilage thickness were considered by a series of computations with various values of h_1. Finally, the effects of age-related changes in overall femoral head compliance (deformation under load) were studied by inputting values of d measured experimentally (35) from pathological load/deflection curves. Unfortunately, experimental data describing detailed spatial perturbations in cartilage and bone stiffness accompanying the changes in h_0, h_1, and d under study were unavailable. It should therefore be noted that the stress distribution changes discussed below result from parametric variations in the loading boundary conditions and not from mesh rezonings or changes in the material property distributions.

RESULTS

1. The Effects of Variations in the Total Hip Load

Consider first the case of an anatomically normal hip in the neutral position, subjected to progressively increasing levels of total joint force F, and undergoing progressively greater deflections d under loading. The F/d relationship used for this simulation series was based upon experimental results for a 44-year hip (16). Anatomical data for the finite element mesh zoning (femoral head radius, neck contour, cancellous bone mechanical properties, etc.) were based upon our own experimental measurements of sections from a fresh-frozen specimen taken from a 50-year-old (body weight = 963 N) at routine autopsy. The cartilage thickness components

h_0 and h_1 for the study section were measured to be 0.8 and 2.0 mm, respectively. These values, along with an unloaded subacetabular gap of 0.76 mm (estimated on the basis of the transition load from Greenwald and O'Connor's force/deflection curve), were taken to be characteristic of a normal hip. These values were input to Eqs. 3–6 in order to calculate the contact stress distribution for various values of F.

Surface loading patterns and internal (femoral head) stress distributions for this normal hip at four different total joint loads (F = 227 to 1810 N) are shown in Fig. 3. The straight lines in the interior are oriented along the calculated principal stress directions and have lengths proportional to the principal stress magnitudes, with solid lines denoting compression and dashed lines representing tension.

It can be seen that contact is incomplete for a 227 N joint force (Fig. 3a). For this reason, the cancellous bone in the "weight bearing" region underlying the acetabular dome has no significant load-bearing function in this case. However, the stresses throughout the femoral head are also noted to be quite small, though by no means uniform. The peak stress level is found to be 0.885 MN/m^2 of compression, and occurs at the distal margin of the

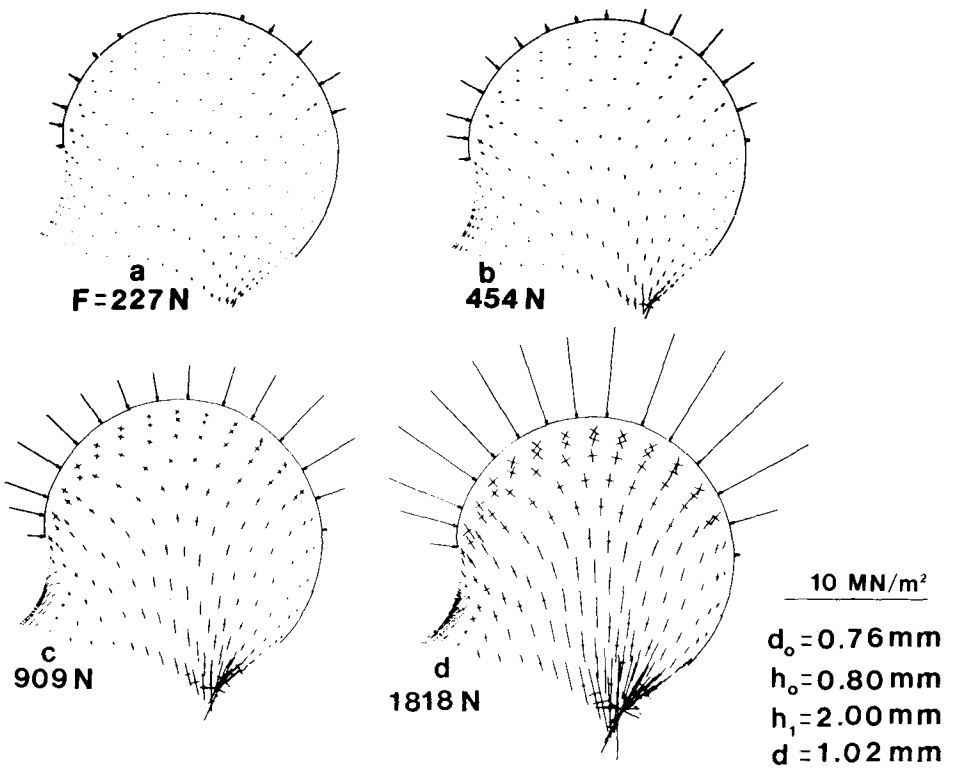

FIGURE 3. The effects of variations in the magnitude of joint force. The arrows arrayed along the articular surface have lengths proportional to the nodal traction forces, which were determined by area integration of the contact stresses calculated from Eq. 3. Note the funnel-like condensation of joint load for transmission to the medical cortex.

medial neck cortex. Very weak tensile stresses (0.1620 MN/m^2) are developed in the lateral neck cortex. When the total joint force is increased to 454 N (Fig. 3b), contact across the articular surface is complete. Although a dye test (7) or a casting test (34) of a hip in this configuration would indicate load transmission at the superior portion of the articular surface, it would be inaccurate to infer that the subjacent cancellous bone is heavily engaged in weight bearing. Indeed, the bone in this region does experience loading, but the stress state is primarily one of transverse, rather than longitudinal, compression. This situation can be seen to result from the presence of peripheral contact stress, which is associated with articular incongruity. Since a vector normal to the articular surface at the periphery ($\phi = \pi/2$) is strongly inclined relative to the resultant force vector, transverse contact stress components must exist at the periphery. With the assumed axisymmetrical loading configuration, the transverse contact stress components are balanced largely by internal transverse compression, rather than by shear stess at the distal (neck) section.

For a total joint load of 909 N (Fig. 3c), the total hip deflection of 1.02 mm in this normal specimen suffices to substantially engage the sub-dome region in weight bearing. The stress state in the underlying cancellous bone is one of roughly equal transverse and longitudinal compression. The joint load is condensed as it funnels along the route of the primary trabecular family, resulting in a point of appreciable (4.765 MN/m^2) stress concentration on the medial cortex. Moderate (1.085 MN/m^2) tensile stresses are observed in the lateral neck cortex, with the neutral axis passing through a point roughly 12 mm lateral to the geometrical neck axis. Because of the relatively high compliance of the medullary region of the neck compared to that of the cortices, the former plays only a minor role in load transmission. Previous numercial simulations (3) have shown that the magnitudes of lateral neck cortex tension can increase fourfold when the angle between the resultant load and the geometrical neck axis is increased by only 30°.

The distribution of surface loading becomes increasingly uniform as the joint force level is increased above the total contact threshold, as is apparent for the case of 1818 N shown by Fig. 3d. The resultant internal stress distribution does not differ appreciably from what would be expected from simple linear extrapolation of that of Fig. 3c. Predictably, the solution was found to become even more linear for higher (3636 N) joint force levels.

2. The Effects of Incongruity Between the Femoral Head and Acetabulum

The degree of anatomical incongruity plays an important role in determining the distribution of contact stress, and hence the stress pattern within the femoral head. This relationship was studied by changing only the value of d_0 (the unloaded subdome gap) in Eqs. 3, 5, and 6, while holding fixed (at the values in Fig. 3c) the joint load, compliance and cartilage thickness parameters (F, h_0, h_1, and d).

It was found that the stress distribution for an almost perfectly congruent hip (d_0 = 0.025 mm, see Fig. 4a) differs very little, on a gross scale, from that for a normally incongruent hip (d_0 = 0.76 mm, Fig. 4b) at this moderate load level. Congruity-induced transverse stress reductions (29% at point *A*) and longitudinal stress augmentations (50% at point *A*) can be detected, however, in the primary trabeculation family. The effects of abnormally high incongruity are, by comparison, much more striking, as illustrated by Figs. 4c (d_0 = 1.02 mm) and 4d (d_0 = 1.27 mm). Superior surface contact is only marginally achieved in the former case, and not at all in the latter. Consequently, the contact stresses necessary to sustain the joint loading are shifted progressively outward toward the periphery of the articular surface. Since contact stress acts normal to the surface in a well-lubricated spherical joint, appreciable transverse compressive stress components are consequently introduced. It can be appreciated from Figs. 4c and 4d that a large portion of the central and superior cancellous bone network is occupied almost solely in supporting these transverse stresses. Indeed, the transverse stresses at point *A* for these two figures are equal to 94% and 113%, respectively, of

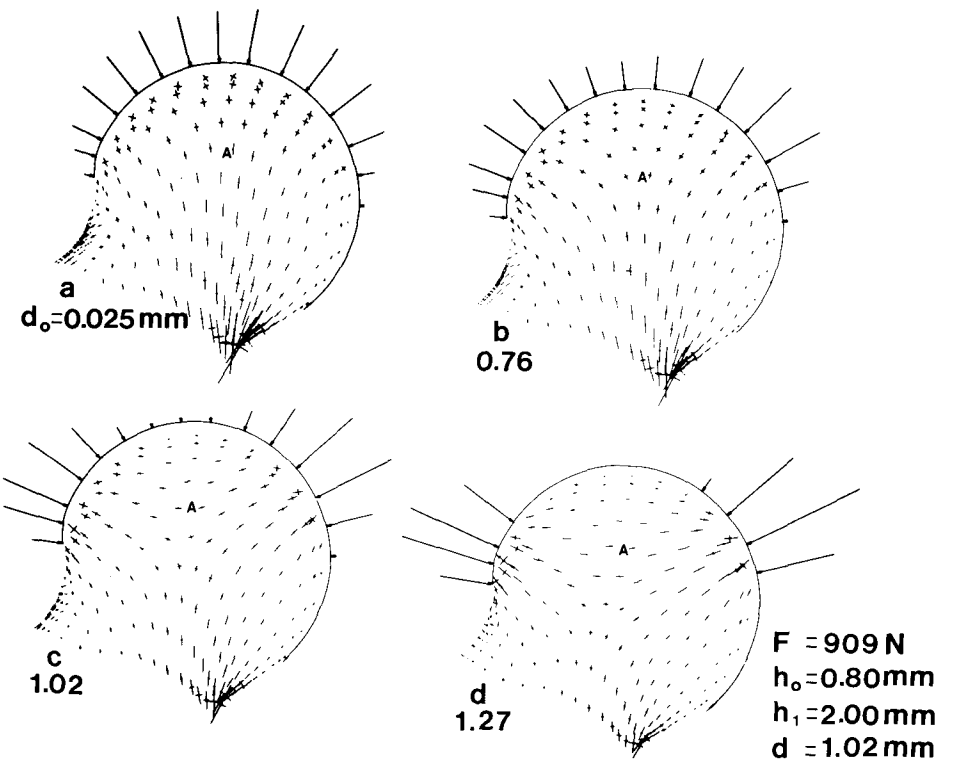

FIGURE 4. The influence of joint incongruity on contact stress patterns and internal stress distribution. A typical point *A* in the primary trabecular family experiences progressive decreases in longitudinal stress and progressive increases in transverse stress as the initial incongruity, d_0, is increased from 0.025 mm to 1.27 mm.

the usual longitudinal stresses at the same point (compare with Fig. 4b). Another interesting consequence of the incongruity increase is a reduction in the relatively small tensile stress magnitudes at the lateral margin of the distal section. In fact, for the extreme case (Fig. 4d) the stress state at this point becomes one of very slight (0.1865 MN/m^2) compression. Coupled with these tension reductions at the lateral margin are comparable reductions in the compressive stress magnitudes at the medial margin.

3. The Effects of Changes in the Overall Cartilage Thickness

A series of computations was undertaken to explore the importance of uniform changes in the cartilage thickness, as reflected by variations of the peripheral (i.e., at $\phi = 90°$) cartilage thickness coefficient. The F, d_0, h_1, and d parameters were held fixed at values characteristic of the normal hip (i.e., as in Fig. 3c), while the value of the h_0 parameter in Eqs. 3–6 was changed. The range of variation in h_0 studied was from 0.025 mm (corresponding to a uniform overall cartilage thickness decrease of 0.77 mm from normal, and implying nearly complete erosion at the periphery) to 4.0 mm (corresponding to very substantial 3.2 mm overall cartilage hypertrophy). It is evident from Fig. 5 that the present model predicts remarkable insensitivity of the stress patterns to parametric changes in h_0. It should

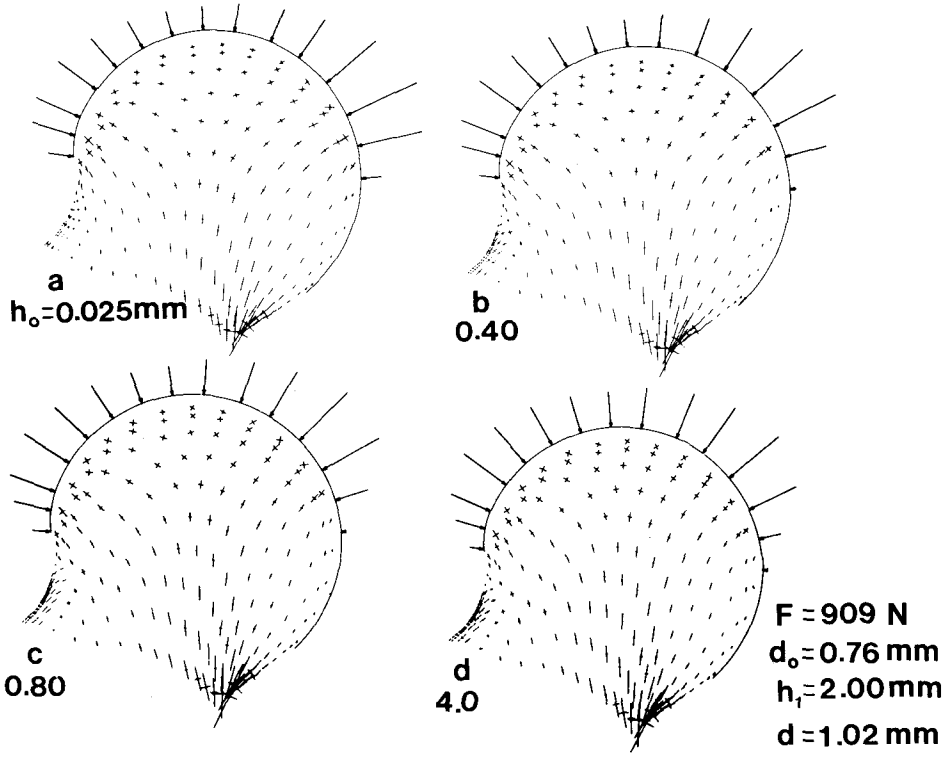

FIGURE 5. Variations in contact load distributions and internal stress patterns caused by increases in the uniform cartilage thickness component, h_0. It can be seen that the processes of load transmission are relatively insensitive to this parameter, provided that the deflection, d, under load remains constant.

be recognized, however, that the requirement that the overall deflection d be held constant as h_0 increases implicitly requires that the cartilage stiffness, a parameter which does not appear explicitly in Eqs. 3–6, must also increase.

4. The Effects of Changes in the Distribution of Cartilage Thickness

The degree of nonuniformity in femoral head articular cartilage thickness distribution is somewhat variable from individual to individual (36). To investigate its role in femoral head stress transmission, computations were performed for various values of the h_1 parameter, while holding fixed the joint load, compliance, incongruity, and the uniform cartilage thickness h_0 in Eqs. 3–6 at normal (i.e., Fig. 3c) values. For reasons similar to those in (*3*) above, the results showed that doubling the normal magnitude of h_1 (i.e., increasing the subdome thickness by roughly two-thirds) produced no appreciable changes in the stress distribution–compare Figs. 6a and 6b. Nor were there any significant changes observed (see Fig. 6c) when h_1 was reduced to nearly zero (perfectly uniform thickness). As h_1 was further decreased into the negative range, corresponding to a cartilage layer which is thicker at the periphery than under the dome, a distinctly different pattern emerged. For constant d, a condition is reached at which the imposed compressive normal strain in the (progressively thinning) subdome cartilage begins to dominate the progressive implicit overall cartilage modulus reductions needed to sustain d as h_1 becomes increasingly negative. Indeed, a singularity arises in Eq. 3 for complete subdome cartilage erosion ($\phi = 0$, $h_1 = -h_0$), a result which is consistent with intuitive expectations and with earlier photoelastic observations (30) of stress elevations occurring due to a reduction in the cushioning capability of the articular cartilage. But local stress elevations within and beneath the thinned subdome cartilage layer cannot occur if large incongruity or small overall compliance prevent complete contact from being achieved. For the otherwise normal hip with only modest subdome erosion (Fig. 6d), the superior "weight-bearing" region is actually the primary load transmission tissue. Although a stress-condensing funnel is still present, its width was markedly reduced, compared to the normal case. The relative magnitude of transverse stress components is small, except in the densely trabecular superior subcortical region. Additional thinning of the cartilage layer produced pronounced compressive stress concentrations in the superior region of the head. For $h_1 = -0.787$ mm (corresponding to a 99% reduction in the subdome cartilage thickness), stresses in some points in this area were increased to more than six times their normal value.

5. The Effects of Changes in the Overall Joint Compliance

Reduced overall compliance of the proximal femur is a well documented attribute of osteoarthritis and rheumatoid arthritis (25, 35). To explore the effects of such changes on stress levels within the femoral head, a series of computations was performed in which the deflection under load, d, was

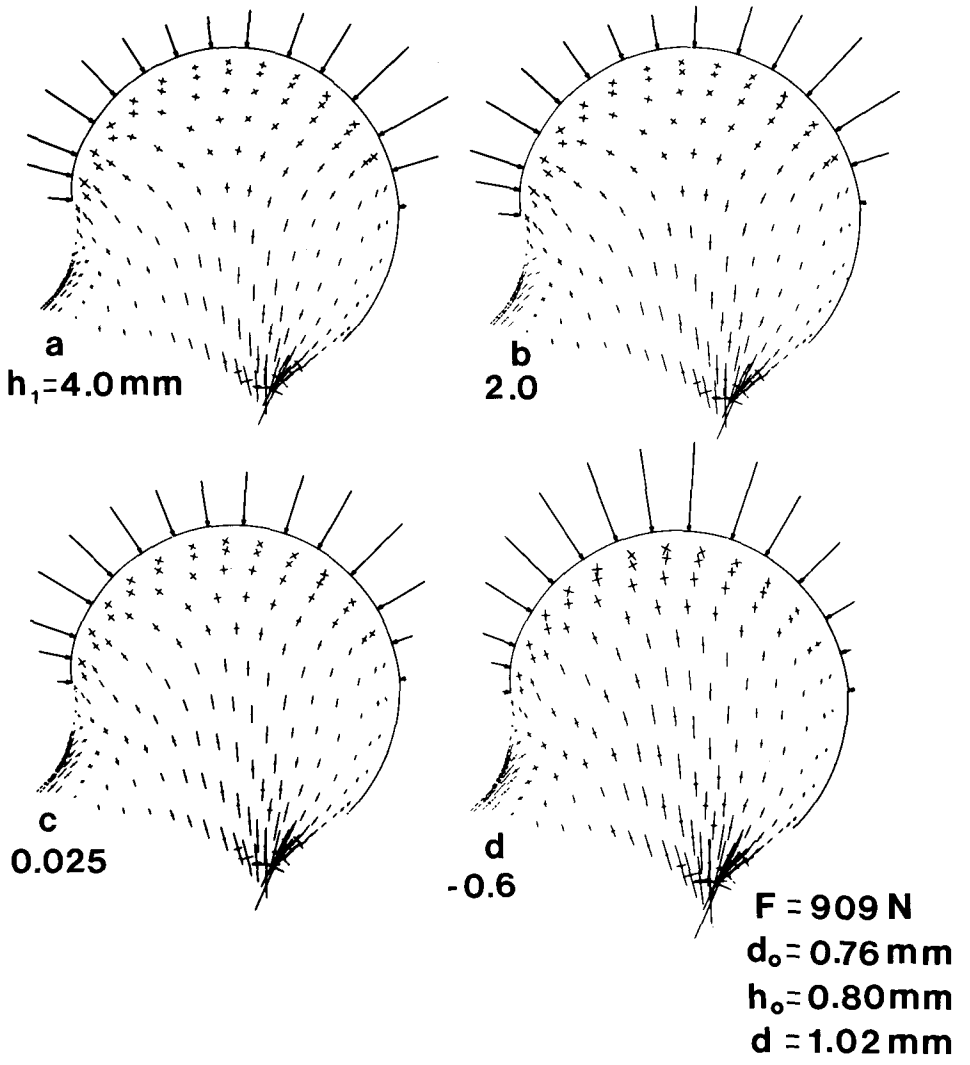

FIGURE 6. The effects of progressive reductions in the nonuniform cartilage thickness component, h_1. Note the progressive increase in the weight-bearing role of the superior region, especially in the case (*d*) of negative h_1. Increases in lateral cortex tensile stresses accompany the increases in medical cortex compressive stresses, and the importance of transverse stress progressively diminishes.

varied accordingly in Eqs. 3, 5, and 6, while F, d_0, h_0, and h_1 were held fixed at normal (see Fig. 3c) values.

As is evident from Fig. 7a, a 25% increase in head compliance relative to normal (Fig. 7b) is relatively inconsequential. By contrast, a 25% decrease in compliance (Fig. 7c) relieves the superior trabeculation of its longitudinal load transmission function. Simultaneously, there is a 25% increase in magnitude and a 10° more transverse change in orientation of the principal stress at the periphery (point *B*). When compliance is further decreased to 50% of normal (Fig. 7d), peripheral stress magnitudes are elevated almost threefold,

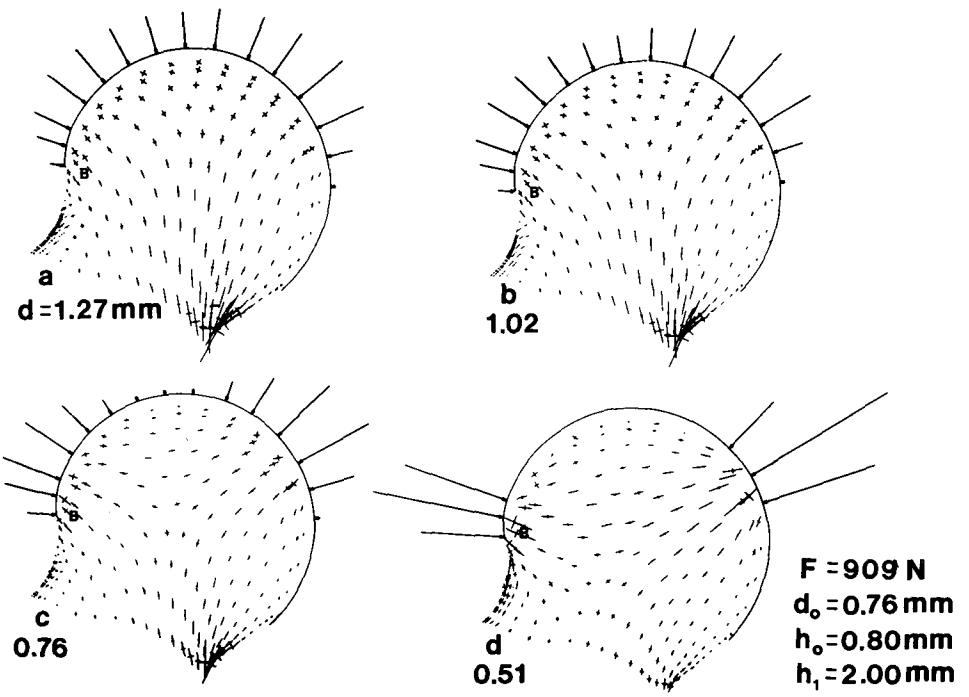

FIGURE 7. The role of reduced overall joint compliance (deflection *d* divided by total force, *F*). The shift of contact stress toward the periphery induces large transverse stresses in much of the central region of the head, as well as strong stress concentrations in the peripheral region (e.g., at point *B*).

and the normal patterns of stress transmission are disrupted in a manner suggestive of, but even worse than, those for a grossly incongruent hip (compare with Fig. 4d).

DISCUSSION

This study addresses the influence of several hip contact abnormalities upon the transmission of stress through the human femoral head. The contact stress distributions, calculated from Greenwald and O'Connor's model (16), are based upon linearly elastic cartilage properties, and involve simplifying geometrical assumptions of perfect femoral head sphericity and sinusoidal cartilage thickness variations. The two-dimensional finite element results approximate the stress distributions in a coronal midsection of the femoral head when it is subjected to the prescribed contact stress patterns at the articular surface and to a zero-displacement boundary condition distally across the neck section. The material properties of the cancellous bone are assumed to be isotropic, linearly elastic, and inhomogeneous, with elastic coefficients varying spatially in accordance with Instron rheological measurements made on a series of autopsy specimens.

Although there is still a lack of direct experimental data with which the calculated stress aberrations might be compared, the results for the medial cortex strain-to-joint-load ratio ($\epsilon_M/F = -2.07\text{x}10^{-6}\text{N}^{-1}$) for the normal

case are in fairly good agreement with the corresponding experimental measurements by Brockhurst ($\epsilon_M/F = -1.66\text{x}10^{-6}\,\text{N}^{-1}$) reported by Valliappan et al. (32). Moreover, the similarity between the trabeculation and principal stress patterns for the normal case (see Fig. 8) suggests that the results of this simplified finite element analysis are at least qualitatively reasonable.

The absence of superior surface contact during the low-load portions of the normal walking cycle is thought to be necessary from the viewpoint of synovial fluid circulation and cartilage nutrition (11, 31). The stress patterns of Figs. 4a and 4b indicate that incomplete contact of this nature does not result in significant load transmission difficulties, because the overall force and stress levels involved are innocuously low. But those factors which impede superior surface contact when the joint load is substantial (e.g., 909 N) will cause serious disruption of the usual patterns of stress transmission.

Under normal conditions of weight bearing, longitudinal compressive stresses are progressively condensed as they funnel distally toward the medial cortex. Small tensile stresses are developed in the lateral region of the neck if the resultant joint loading force passes outside the medial cortex of the neck (22). Anatomically, the primary trabecular family appears to be adapted distally to nearly uniaxial compression, and proximally to an essentially shear-free equibiaxial compression state. The present model indicates that when superior surface contact is prevented at substantial load levels, the burden of weight bearing must shift to the peripheral contact regions. The adverse consequences of this contact stress redistribution in a well-lubricated joint involve not only stress concentration due to reduced contact area (a relatively minor problem), but also the introduction of large transverse compressive stresses. Under such conditions, the femoral head is loaded somewhat in the manner of an inverted keystone, with the transverse compressive stresses in the superio-central region substantially exceeding in magnitude

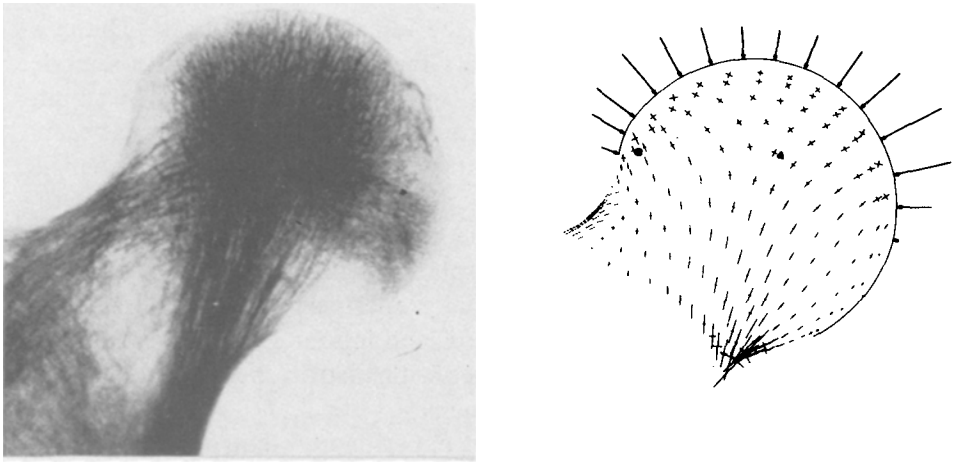

FIGURE 8. A comparison of the trabeculation pattern (left) and principal stress pattern (right) for a normal femoral head in the neutral position. The role of the arcuate (tensile or secondary) trabeculation system becomes increasingly important in abduction and varus (3).

those which are required for longitudinal load transmission in the normal hip. Clearly, changes of this nature should constitute a strong stimulus for architectural remodelling in the femoral head. The relative magnitude of the transverse stresses will be diminished, however, if the femoral head is not fully recessed within the acetabulum (i.e., if $\phi < 90°$ at the periphery) during loading.

The parametric variations studied computationally indicate that substantial adverse changes in the patterns of weight bearing can result from hip incongruities only 0.5 mm greater than normal (compare Figs. 4b and 4d), but that comparably reduced incongruities are (from a load transmission viewpoint) relatively benign. Changes in the overall cartilage thickness, if such changes can be assumed to occur in isolation from changes in the overall femoral head compliance [unfortunately, an improbable circumstance–Simon, (28)], will have no appreciable effect on the stress patterns in the head. A cartilage layer which is substantially thicker than normal superiorly does not markedly alter the loading pattern for moderate joint force, but would be expected to slightly lower the force level at which the transition to a linear load/deflection curve occurs (16). However, a cartilage layer which is substantially thinner than normal superiorly is subject to appreciable stress concentrations.

Decreases in the overall femoral head compliance, such as those which result from the cartilage thinning and/or subchondral bone sclerosis characteristic of osteoarthritis, were found to have much the same effects on load transmission as does enhanced incongruity. That is, complete articular contact is impossible at moderate or high loads, resulting in the introduction of large transverse stresses at the periphery. The resultant aberrant stress patterns, if continued over long periods, could constitute a strong remodelling stimulus, and may thus contribute to the trabecular restructuring and peripheral osteophyte formation commonly observed in hip osteoarthritis (see Fig. 9).

The thin trabecular struts which run perpendicular to the main load bearing trabecular sheets (23) may be helpful in preventing sheet buckling for longitudinally-loaded cancellous bone, but it is unlikely that such an arrangement would be well adapted to sustaining abnormally high levels of transverse compression. Our laboratory measurements of the spatial variations and the anisotropic characteristics of the yield strength of femoral head cancellous bone (4) indicate that, as a rough approximation, the primary trabeculation system can safely bear transverse stress at only half the level which can be sustained longitudinally. Especially under cyclic loading conditions, contact stress aberrations which magnify transverse stress levels in the interior of the head could lead to an increased incidence of trabecular strut fatigue fractures, and hence to hypervascularity and cyst formation (12). Indeed, the regions most prone to trabecular fracture in the osteoarthritic hip (17) seem to correlate with those shown here to be subject to transverse stress elevations.

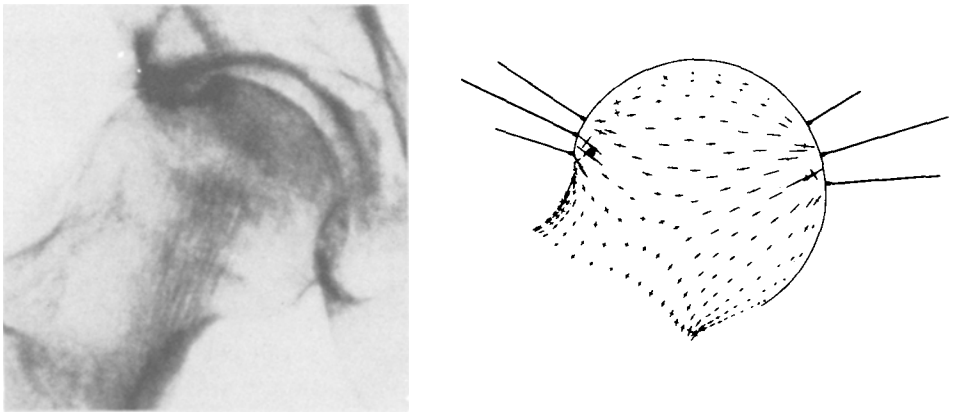

FIGURE 9. Radiograph of an osteoarthritic hip (left) compared with stress patterns in a hip with abnormally high stiffness. The cartilage thickness reductions and degenerative changes at the periphery correlate with areas of calculated stress concentrations.

CONCLUSIONS

The results of this study demonstrate that the patterns of stress within the femoral head are strongly dependent upon the articular contact stress distribution. Clearly, the accuracy of structural analyses of the major articular joints would be markedly enhanced by the availability of actual contact stress data. For the present model of the femoral head, most of the articular cartilage thickness changes and contour changes considered were relatively insignificant, provided that changes in the overall joint compliance were not involved. However, both abnormally large hip incongruity and abnormally low hip compliance can result in the development of large transverse compressive stresses throughout much of the femoral head. At best, these transverse stresses do little to enhance the weight-bearing capabilities of the hip. At worst, they may contribute to trabecular fatigue fractures, hypervascularity, sclerosis, cyst production, and peripheral osteophyte formation.

REFERENCES

1. Andriacchi, T.P., J.O. Galante, T.B. Belytschko, and S. Hampton. A stress analysis of the femoral stem in total hip prostheses. *J. Bone J. Surg.* 58A: 618-624, 1976.
2. Blowers, D.H., R. Elson, and E. Korley. An investigation of the sphericity of the human femoral head. *Med. Biol. Eng.* 10, 762-775, 1972.
3. Brown, T.D., and A.B. Ferguson, Jr. The development of a computational stress analysis of the femoral head–mapping tensile, compressive and shear stress for the varus and valgus positions. *J. Bone J. Surg.* 60A: 619-629, 1978.
4. Brown, T.D., and A.B. Ferguson, Jr. Mechanical property distributions in the cancellous bone of the human proximal femur. *Acta Orthop. Scand.* 1980. In press.
5. Brown, T.D., and D.R. Muratori. Miniature piezoresistive transducers for transient soft-body contact stress problems. *Exp. Mech.* 19: 214-219, 1979.

6. Bullough, P., J. Goodfellow, A.S. Greenwald, and J. O'Connor. Incongruent surfaces in the human hip joint. *Nature* 217: 1290, 1968.
7. Bullough, P., J. Goodfellow, and J. O'Connor. The relationship between degenerative changes and load bearing in the human hip. *J. Bone J. Surg.* 55B: 746-758, 1973.
8. Crowninshield, R.D., R. A. Brand, and R.C. Johnston. An analysis of femoral stem design in total hip arthroplasty. Proceedings of the 25th Annual Meeting of the Orthopaedic Research Society, 1979, p. 33.
9. Day, W.H., S.A.V. Swanson, and M.A.R. Freeman. Contact pressures in the loaded human cadaver hip. *J. Bone J. Surg.* 57B: 302-313, 1975.
10. Ergatoudis, I., B.M. Irons, and O. C. Zienkiewicz. Curved, isoparametric 'quadrilaterial' elements for finite element analysis. *Int. J. Solids Struct.* 4: 31-42, 1968.
11. Freeman, M.A.R. *Adult Articular Cartilage,* edited by M.A.R. Freeman. New York: Grune and Stratton, 1972.
12. Freeman, M.A.R. The pathogenesis of primary osteoarthritis: An hypothesis. In: *Modern Trends in Orthopaedics - 6,* edited by A.G. Apley. London: Butterworths, 1972.
13. Freeman, M.A.R., W.H. Day, and S.A.V. Swanson. Fatigue fracture in the subchondral bone of the human cadaver femoral head. *Med. Biol. Eng.* 9: 619-629, 1971.
14. Greenwald, A.S. Joint congruence–a dynamic concept. In: Proceedings of the Second Open Scientific Meeting of the Hip Society, edited by W.H. Harris. St. Louis: C.V. Mosby, 1974.
15. Greenwald, A.S., and D.W. Haynes. Weight-bearing areas in the human hip joint. *J. Bone J. Surg.* 54B: 157-163, 1972.
16. Greenwald, A.S., and J.J. O'Connor. The transmission of load through the human hip joint. *J. Biomech.* 4: 507-528, 1971.
17. Griffiths, W.E.G., S.A.V. Swanson, and M.A.R. Freeman. Experimental fatigue fracture of the human cadaveric femoral neck. *J. Bone J. Surg.* 53B: 136-143, 1971.
18. Harris, L.J., R. Chao, and R. Bloch. A three-dimensional finite element analysis of the proximal third of the femur. Proceedings of the 24th Annual Meeting of the Orthopaedic Research Society, 1978, p. 16.
19. Irons, B. M. Quadrature rules for brick based finite elements. *Int. J. Numerical Meth. Eng.* 3: 293-294, 1971.
20. Kempson, G.E., C.J. Spivey, S.A.V. Swanson, and M.A.R. Freeman. Patterns of cartilage stiffness on normal and degenerate human femoral heads. *J. Biomech.* 4: 597-609, 1971.
21. Paul, J.P. Forces transmitted by joints in the human body. *Proc. Inst. Mech. Eng.* 181: 8, 1967.
22. Pauwels, F. *Biomechanics of the Normal and Diseased Hip.* New York: Springer Verlag, 1976.
23. Pugh, J.W., R.M. Rose, and E.L. Radin. A structural model for the behavior of trabecular bone. *J. Biomech.* 6: 657-670, 1973.
24. Radin, E.L., I.L. Paul, and D. Pollack. Animal joint behavior under excessive load. *Nature* 226: 554-555, 1970.
25. Radin, E.L., I.L. Paul, and R.M. Rose. The role of mechanical factors in the pathogenesis of primary osteoarthritis. *Lancet.* 1: 519-521, 1972.
26. Rybicki, E.F., F.A. Simonen, and E.B. Weis. On the mathematical analysis of stress in the human femur. *J. Biomech.* 5: 203-215, 1972.
27. Scholten, R., H. Rohrle, and W. Sollbach. Analysis of stress distribution in natural and artifical hip joints using the finite element method. *S. Afr. Mech. Eng.* 28: 220-225, 1978.
28. Simon, W.H. Scale effects in animal joints. II. Thickness and elasticity in the deformability of articular cartilage. *Arthritis Rheum.* 14: 493-502, 1971.
29. Simon, B.R., G.M. Stanley, H.A. Kamel, and L.F. Peltier. Relation of subchondral bone and articular cartilage stresses to joint function. Proceedings of the 5th International Conference on Experimental Stress Analysis, 1974, pp. 343-351.
30. Spivey, C.J., and H. Muir. Some biomechanical and biochemical abnormalities in the articular cartilage of femoral heads displaying marked osteoarthritic change. *J. Bone J. Surg.* 53B: 149, 1971.
31. Torzilli, P. A., and V. C. Mow. On the fundamental fluid transport mechanism through normal and pathological articular cartilage during function. II. The analysis, solution, and conclusions. *J. Biomech.* 9: 587-606, 1976.
32. Valliappan, S., N.L. Svensson, and R.D. Wood. Three dimensional stress analysis of the human femur. *Comput. Biol. Med.* 7: 253-264, 1977.

33. Walker, P.S., D. Dowson, M.D. Longfield, and V. Wright. Boosted lubrication in synovial joints by fluid entrapment and enrichment. *Ann. Rheum. Dis.* 27: 512-520, 1968.
34. Walker, P.S., and M.J. Erkman. The role of the menisci in force transmission across the knee. *Clin. Orthop. Relat. Res.* 109: 184-192, 1975.
35. Walker, T.W., J.D. Graham, and R.H. Mills, Changes in the mechanical behavior of the human femoral head associated with arthritic pathologies. *J. Biomech.* 9: 615-624, 1976.
36. Woods, C.G., A.S. Greenwald, and D.W. Haynes. Subchondral vascularity in the human femoral head. *Ann. Rheum. Dis.* 29: 138-142, 1970.
37. Zienkiewicz, O.C. *The Finite Element Method* (3rd ed.) London: McGraw-Hill, 1977.